Journal Pre-proof

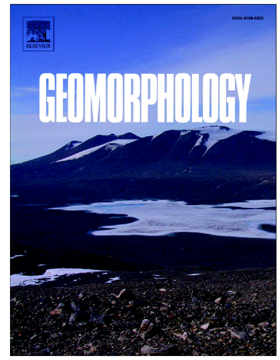

Primary drivers of dune cover and shoreline dynamics: A conceptual model based on the Iberian Atlantic coast

Rita González-Villanueva, Martiño Pastoriza, Armand Hernández, Rafael Carballeira, Alberto Sáez, Roberto Bao

PII: S0169-555X(22)00449-4

DOI: https://doi.org/10.1016/j.geomorph.2022.108556

Reference: GEOMOR 108556

To appear in: *Geomorphology*

Received date: 13 March 2022

Revised date: 7 December 2022

Accepted date: 7 December 2022

Please cite this article as: R. González-Villanueva, M. Pastoriza, A. Hernández, et al., Primary drivers of dune cover and shoreline dynamics: A conceptual model based on the Iberian Atlantic coast, *Geomorphology* (2022), https://doi.org/10.1016/j.geomorph.2022.108556

PRIMARY DRIVERS OF DUNE COVER AND SHORELINE DYNAMICS: A CONCEPTUAL MODEL BASED ON THE IBERIAN ATLANTIC COAST

González-Villanueva, Rita[1*]; Pastoriza, Martiño[1]; Hernández, Armand[2]; Carballeira, Rafael[2], Sáez, Alberto[3]; Bao, Roberto[2]

[1]Centro de Investigación Mariña, Universidade de Vigo, XM-1, 36310 Vigo, España

[2] Universidade da Coruña, GRICA Group, Centro Interdisciplinar en Química e Bioloxía (CICA), Facultade de Ciencias, Rúa as Carballeiras, 15071, A Coruña, España

[3] UB-Geomodels Research Institute, Dep. Dinàmica de la Terra i de l'Oceà, Universitat de Barcelona, Marti i Franqués, s/n 08028, Barcelona, España

*Corresponding author: Centro de Investigación Mariña, Universidade de Vigo, XM-1, 36310 Vigo, España. E-mail address: ritagonzalez@uvigo.es

KEYWORDS

Coastal dune evolution, shoreline change, ground-penetrating radar, wind stilling, sea level rise, storminess

1. INTRODUCTION

A large percentage of the world's population is located in coastal zones (Small and Nicholls, 2003). In the European Union, 19% of the population lives within 10 km of the coast (EEA, 2006). Depositional coasts, such as those containing dune systems, are essential geomorphic systems that protect populations and infrastructure from natural coastal hazards by absorbing energy and momentum fluxes from the ocean (Arkema et al., 2013). However, these systems are highly vulnerable to storms and particularly the erosion and flooding associated with wave inundation and storm surge. Considering that both sea-level rise and storm-track variations are linked to climate change (Fortunato et al., 2019; Walsh et al., 2016), dune stability should be a worldwide concern, as the existing hazards in these highly populated areas are expected to be intensified in the future (Kirezci et al., 2020; Oppenheimer et al., 2019). Foredunes, which are parallel to shore ridges that are formed above the limit of non-storm waves, are crucial in acting as the first line of defense against flooding of the hinterland (Arkema et al., 2013; Barbier et al., 2011; Vousdoukas et al., 2020). Thus, an improved understanding and awareness of the effects of coastal hazards on foredune systems is crucial for preventing further environmental degradation, improving safety, and reducing the impacts of hazards on coastal populations.

Extensive research has shown that dunes evolve in response to changes in sediment supply and vegetation cover. In turn, these changes also depend on waves and winds, the primary sediment transport process drivers (Hesp, 2002; Murray et al., 2008; Zarnetske et al., 2015). Both of these drivers also condition the shoreline, one of the most dynamic features of coasts, which has been used in a broad range of studies analyzing the coastal erosion-accretion trends worldwide (Boak and Turner, 2005; Castelle et al., 2022; Costas et al., 2006; Vousdoukas et al., 2020). However, there is a general paucity of studies describing how landscape dune evolution and shoreline dynamics are interrelated. Under accelerated climate change scenarios and their resulting sea-level rise, disentangling the relative importance of waves and wind on coastal dune behavior and shoreline dynamics is crucial for assessing future coastal vulnerability and geomorphic stability.

The present work aims to shed light on the landscape evolution of coastal dunes and explore the primary drivers that control their short-to long-term episodic deterioration and recovery. In this study, we perform a multiapproach analysis of a coastal dune system on the Atlantic NW Iberian coast (Doniños coastal dunes) over the last 70 years under minor human impacts. From this case study, we aim to examine the coastal dune landscape evolution processes that are linked to wind and marine regimes on the decadal scale. This paper has two key aims: (i) to evaluate the relationship between shoreline and dune landscape changes since the mid-20th century and (ii) to establish the role of wind and wave variability on the processes that lead to the observed effects.

2. ENVIRONMENTAL SETTING

The Doniños sandy system is located on the NW rocky coast of the Iberian Peninsula (Spain; Figure 1). This area was a semirestricted military area from the 18th century until 1996. Currently, it is a Site of Community Importance established under the Habitats Directive of the EU (Special Area of Conservation (SAC) ES1110002 and Special Protection Area (SPA) ES0000258).

The Doniños coastal system comprises a 1.7-km-long and 400-m-wide sandy barrier with a NNE-SSW orientation and is anchored to rocky outcrops at both ends (Figure 1). The barrier confines a perched freshwater lake, to the east, which formed 4.5 kyr BP, during the last highstand period. Stratigraphic and sedimentological data indicate that the sandy barrier experienced several breaching episodes during the late Holocene (Sáez et al., 2018). The connection between the backbarrier area and the sea has been restricted in recent decades and occurs through a 1 km meandering channel, and the characteristics of the drainage channel slope and section hinder the flow of seawater into the backbarrier. On the other hand, the outflow channel activity is linked to episodes of maximum water levels in the lake that occur with extreme rainfall events, as documented in other systems of the Galician region (González-Villanueva et al., 2017; Vilas and Rolán, 1985). As a result, sediment transfer through the channel can be considered negligible at a decadal time scale.

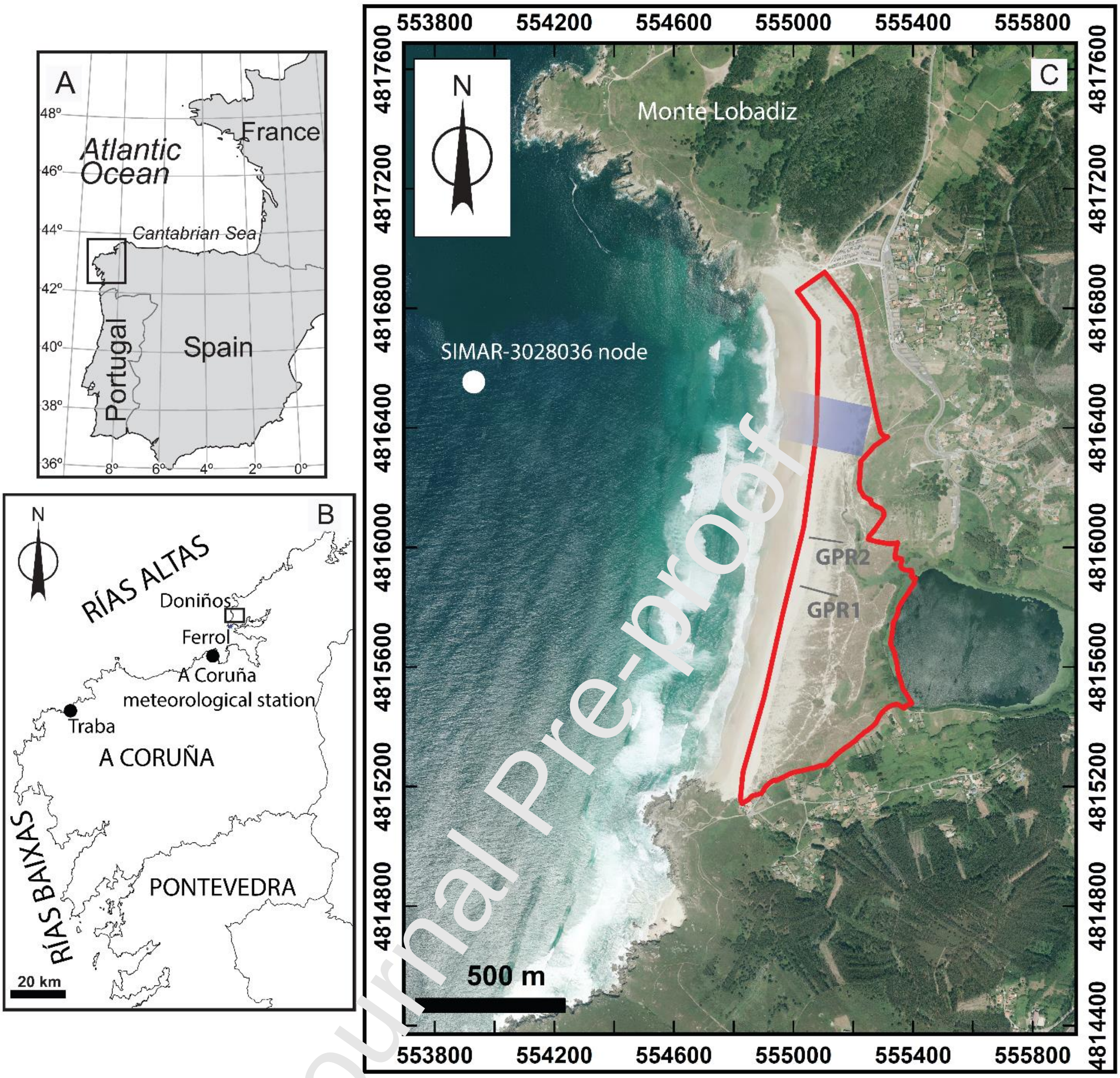

Figure 1. (A-B) Location of the study site on the Iberian Peninsula (C) Aerial imagery of the Doniños coastal system (2017); the white dot indicates the location of the SIMAR-3028036 node, the red polygon denotes the fixed area used to calculate vegetation cover changes, the blue shaded area corresponds to the outlet area of the drainage channel, and the gray lines indicate the positions of the GPR sampling transects.

The coastal barrier separates the lake from the sea and comprises two different geomorphological units, namely, the beach and the dune. The foredune is sparsely vegetated, and its crest reaches elevations higher than 13 m above mean sea level in Alicante (MSLA; topographic Spanish Zero, located 1.88 m above mean sea level at the Ferrol maritime port; see www.puertos.es for more information). The backdune has dense vegetation cover and an irregular topography with large depressions reaching depths of 4.5 m above the MSLA.

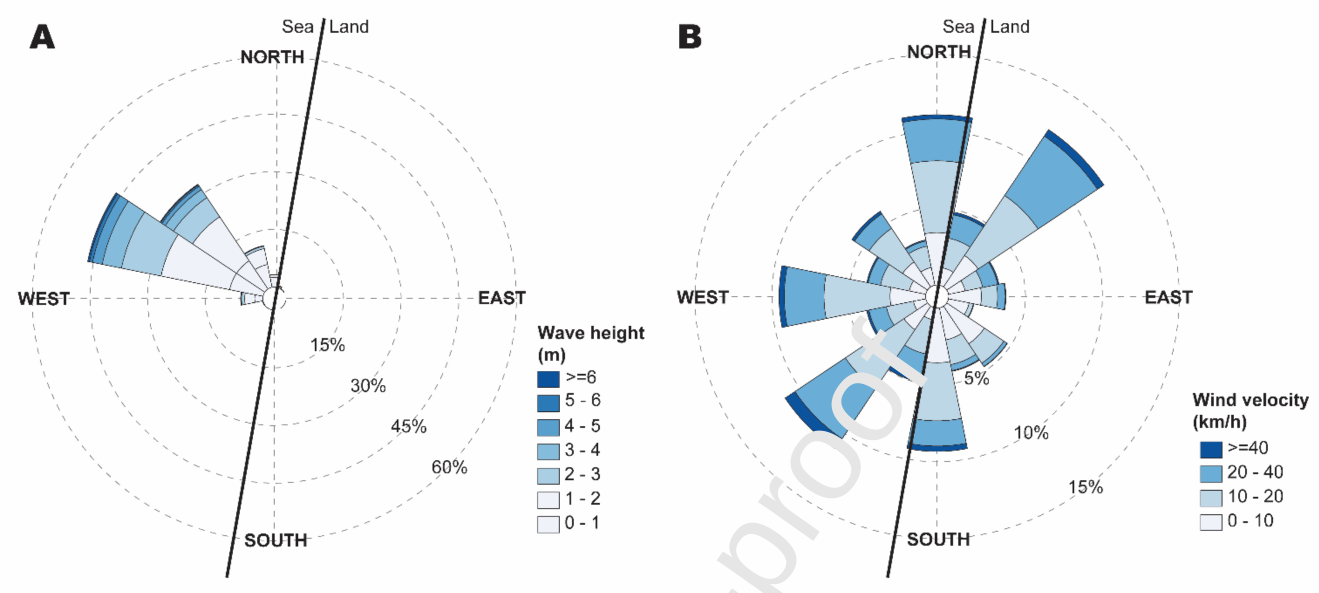

Figure 2. (A) Diagram showing the significant wave height (H_s) measured at the SIMAR-3028036 node between 1958 and 2020 (data source: Puertos del Estado). (B) Diagram showing the wind velocity (km/h) measured at A Coruña meteorological station between 1938 and 2020 (data source: Agencia Estatal de Metereología). The continuous black line indicates the coastline orientation from 190° (SSW) to 10° (NNE).

The coast is under a mesotidal regime, with a spring tidal range of 4.45 m. The local mean sea level (MSL) is approximately 4.24 m above the MSLA, and the highest astronomical tide (HAT) is approximately 6.48 m above the MSLA. High waves come from the W to NW directions, with the greatest wave heights reaching between 6 and 10 m. The NNE-SSW orientation of the system makes the sand barrier vulnerable to the direct impacts of these energetic waves (Figure 2). The prevailing winds in the area are dominated by N, NE, W and SW components, and the strongest onshore winds blow from the SW direction and directly impact the study area (Figure 2).

3. MATERIALS AND METHODS

In this work, we investigated the Doniños coastal dune system, using a multiproxy approach combining aerial imagery, topographic data, ground-penetrating radar (GPR) profiles, and meteorological and oceanographic (metocean) data.

3.1 Aerial imagery: *Coastal dune landscape and shoreline changes*

Fourteen historical aerial photographs and orthophotographs taken from 1945 to 2020 (Table 1), with spatial scales ranging from 1:20000 to 1:5000, were used to analyze the vegetation cover variations, coastal dune growth, reactivation, stabilization, and shoreline changes in the study area. These aerial photographs were georeferenced to the most recent orthophotograph (2020) using the ETRS89-UTM29N (EPSG:25829) reference system in geographic information system software (ArcGIS 10.3). After calibration points were selected, a transformation model was used to compute the georeferenced image coordinates and associated mean quadratic error. This error was systematically set to be below 5 m, except in 1945, when the accepted error was less than 10 m due to the low image quality.

Table 1. Sources of the aerial photographs and orthophotographs used in this work, including the date (month/year), type, source, and georeferenced error of each photograph. In the "type" column, O indicates an orthophotograph and AP indicates an aerial photograph. Sources: Centro Nacional de Información Geográfica (CNIG) and Centro Cartográfico y Fotográfico –Ejército del Aire (CECAF).

DATE	TYPE	SOURCE	ERROR (m)	DATE	TYPE	SOURCE	ERROR (m)
6/2020	O	CNIG	-	**9/2002**	O	CNIG	-
6/2017	O	CNIG	-	**7/1990**	AP	CNIG	3,8
7/2014	O	CNIG		**7/1986**	AP	CNIG	4,8
8/2010	O	CNIG	-	**9/1984**	AP	CNIG	0,6
7/2008	O	CNIG	-	**5/1976**	AP	CECAF	4,5
6/2005	O	CNIG	-	**10/1956**	O	CNIG	-
4/2003	AP	CNIG	1,1	**10/1945**	AP	CECAF	9,3

Given that the long-term shoreline change in the beach-dune system according to historical aerial photographs was addressed in this work, the limit between the vegetated dune and the beach was selected as the shoreline indicator (Boak and Turner, 2005). This demarcation was consistent with previous shoreline change studies (Anderson et al., 2014; Castelle et al., 2018; Costas et al., 2006) and was manually digitized in a shapefile format on each available date. In 2020, this demarcation was also mapped using a real-time kinematic global positioning system (GPS-RTK) (Trimble R10). The shoreline was divided into south and north sections, avoiding the area with inlet dynamics. The shoreline changes were analyzed using version 5.0 of the Digital Shoreline Analysis System (DSAS) tool (Himmelstoss et al., 2018). The baseline was drawn at a 500 m distance landward, parallel to the shoreline orientation. Seaward transects of a 1 km length each and an equal spacing of 10 m along the baseline, were generated through the DSAS software. Thus, the entire Doniños shoreline, except for the area affected by the channel discharge outlet, was represented by 160 transects that were perpendicular to the baseline.

The overall coastal system was then divided into six surficial environmental units: (i) the unvegetated area, (ii) dune vegetation, (iii) marsh vegetation, (iv) the flooded area, (v) rocky outcrops, and (vi) anthropic infrastructure. These units were identified and manually digitized on a series of aerial images using ArcGIS software to obtain the extensional changes that occurred during the studied period, and changes in the vegetated unit percentage of the dunes were estimated relative to a fixed polygon covering the area of interest (Figure 1). The available aerial images (Table 1) corresponded to the summer season (April to September in the study area) except in 1945 and 1956, in which the images corresponded to the first days of winter, October 8th and 13th, respectively. However, to minimize any seasonal change, a trend line and 99.5% confidence limit of the percent temporal vegetation cover values were obtained.

3.2 GPR: *Imprints of extreme events in foredunes*

GPR is a valuable and noninvasive geophysical tool to study the internal structures of coastal dunes (Bristow et al., 2000; Costa et al., 2016; Girardi and Davis, 2010; González-Villanueva et al., 2013). A GPR system with a 200-MHz antenna from Geophysical Survey Systems, Inc. (GSSI) was used to image the subsurface; this antenna was synchronized to a GPS-RTK. Two 2D profiles were registered along cross-shore transects to record the recent foredune evolution observed in the available aerial imagery (Figure 1). The radar profile acquisition was optimal, and a backshore analysis was possible due to the salt-water signal loss. GPR data were acquired in September 2019, at a 0.1-m interval between traces and a frequency of 0.25 samples/ns. These data were processed using Sandmeier REFLEXW software following the sequential steps proposed by Neal (2004) (including zero-time correction, signal-saturation correction, gains and filter application, static correction and migration steps). The radar-wave velocities were calculated using the interactive hyperbola-adaptation method. A velocity of 0.12 m/ns was estimated for the profiles corresponding to dry sand; this velocity matches the expected values found in the literature (Costas et al., 2006; González-Villanueva et al., 2013; Reynolds, 1997; Robin et al., 2021). Once the data were processed, a GPR data interpretation was undertaken using the Kingdom SMT software by cross-cutting the radargrams with information on the shoreline position derived from the aerial imagery analysis and the topographic profiles at the same location in 2010 and 2015 (0.5 m resolution) which were obtained from digital elevation models (DEM) derived from the light detection and ranging (LiDAR) data downloaded from the Centro Nacional de Información Geográfica (CNIG) (https://centrodedescargas.cnig.es).

3.3 Metocean data: *Establishing the variabilities in forcing conditions*

The after-effects of metocean forces on recent coastal dune evolution were evaluated using publicly available data sets that overlapped with the study period (Table 2). We examined the wind and wave regimes to explore the existence of any decadal or seasonal (winter-summer) variability or trends during the study period. Winter was defined as be the period between October and March, while summer was defined as that from April to September. The utilized meteorological data set included wind parameters that were derived from a near-coastal meteorological station, A Coruña, which is located 16 km south of the Doniños system (Figure 1), whereas the wave climate data from the SIMAR-3028036 node located 900 m seaward at a 14 m water depth (Figure 1) included significant wave height, period, and directional data.

Table 2. Summary of the available metocean data.

TYPE OF DATA	UNIT	TEMPORAL RESOLUTION	TEMPORAL RANGE	DATA SOURCE
WIND	m s^{-1}	6 hour 1 hour	1931-1990 1990-2020	Agencia Estatal de Meteorología
OFFSHORE WAVES (H, T, DIRECTION)	(m, s, °)	1 hour	1958-2020	Puertos del Estado

Due to the shape and orientation of the coast and the distance of the node to the study area (Figure 1), offshore wave data derived from a hindcast time series model (SIMAR-3028036 node, Puertos del Estado) were directly used to discover storm events that may have been responsible for dune retreat. Notably, that the values on the studied beach were almost certainly higher due to wave run-up. To extract storm events, we first filtered the data to consider only onshore waves (from 190° (SSW) to 10° (NNE)). Then, following the methods of Masselink et al. (2014) and Castelle et al. (2015), a threshold corresponding to the 95th percentile of the offshore significant wave height ($H_{s95\%}$ =4.12 m) was used to retrieve the storm events. A single storm event was defined as the period when H_s>$H_{s95\%}$ during at least one complete tidal cycle (12 h). In a succession of two or more storms, if the 'calm' or 'still' period between the events was less than 5 days, it was considered a cluster of storms. In addition, following the criteria proposed by Lorente et al. (2018) for NW Spain, when the Hs exceeds the 99th percentile ($H_{s99\%}$ = 5.55 m), the event was considered an extreme-energy event.

Onshore wave data were used to estimate the potential impact of waves on coastal dunes through the calculation of the onshore seasonal (winter and summer) longshore P(x) and cross-shore P(y) components of the wave power, using a simplification of the Komar (1976) equation based on the linear wave theory, which has been used in previous studies (Herrero et al., 2020; McCormick. and Kraemer, 2001), and is expressed as follows:

$$\begin{cases} P(x) = H_s^2 T_p \sin\varphi \\ \mathrm{P(y)} = H_s^2 T_p \cos\varphi \end{cases} \quad (1)$$

where T_p is the peak period (s) and φ is the angle between the wave direction and the perpendicular direction of the coastline (degrees).

The seasonal wind conditions and potential for aeolian sand transport were estimated using the A Coruña meteorological station wind records between 1938 and 2020. In this wind analysis, only onshore-directed winds were considered (from 190° (SSW) to 10° (NNE)), as these were the only winds responsible for transporting particulate sediment from the beach to the dune. Equation (2), which was proposed by Bagnold (1936) was used to calculate the wind shear velocity threshold, above which aeolian sand transport occurs, which is expressed as follows:

$$v_{t*} = A \sqrt{D\ g \frac{(\rho_s - \rho)}{\rho}} \quad (2)$$

Where v_{t*} is the velocity threshold for motion (m/s); A is an empirical coefficient (nominal value of 0.08); D is the grain diameter (m) in the study area, which was set to 0.3 mm and corresponds to the dune mean grain size; g is the gravitational acceleration (9.81 m/s^2); ρ_s is the sand grain density (kg/m^3); and ρ is the air density (kg/m^3). Using the obtained shear wind velocity values, the critical movement initiation velocity at an elevation of 10 m was calculated using the v_{10crit} equation (3) proposed by Bagnold (1936), which is expressed as follows:

$$v_{10crit} = 5.75\ v_{t*} \log \frac{Z}{Z'} \quad (3)$$

where Z is the elevation at which the wind velocity is determined (m) and Z' is the surface roughness height (m), which is considered equal to D/30, after Bagnold (1941). Using equation (3), the number of events exceeding the motion threshold was obtained. Additionally, the sediment transport potential per year was estimated by applying the aeolian sediment transport model developed by Bagnold (1936) as follows:

$$Q = \left(\frac{k}{\ln \frac{Z}{Z'}}\right)^3 C\ \frac{\rho}{g} \sqrt{\frac{D}{D_{ref}}}\ (v_{10} - v_{10crit})^3 \quad (4)$$

where k is the Prandtl-Von Karman constant ($k \approx 0.4$), and C is a parameter accounting for the grain size distribution width, which ranges from 1.5 to 2.8 (Bagnold, 1941). Here C is set to 2.8, the highest value of beach sediment heterogeneity, and D_{ref} corresponds to the standard sand grain size (0.25 mm).

4. RESULTS

4.1 Shoreline changes and extreme-event imprints

Overall, the position of the shoreline showed seaward migration over 1945-2020, with an average advance rate of 1.28±0.01 m/year (Figure 3). In particular, considerable shoreline retreat occurred within three periods, namely, 1986-1990, 2002-2003 and 2008-2017, in which over 70% of the shoreline experienced erosion at an average rate greater than 2 m/year (Figure 4). In general, shoreline retreat was more prominent in the southern sector than in the other regions during these periods.

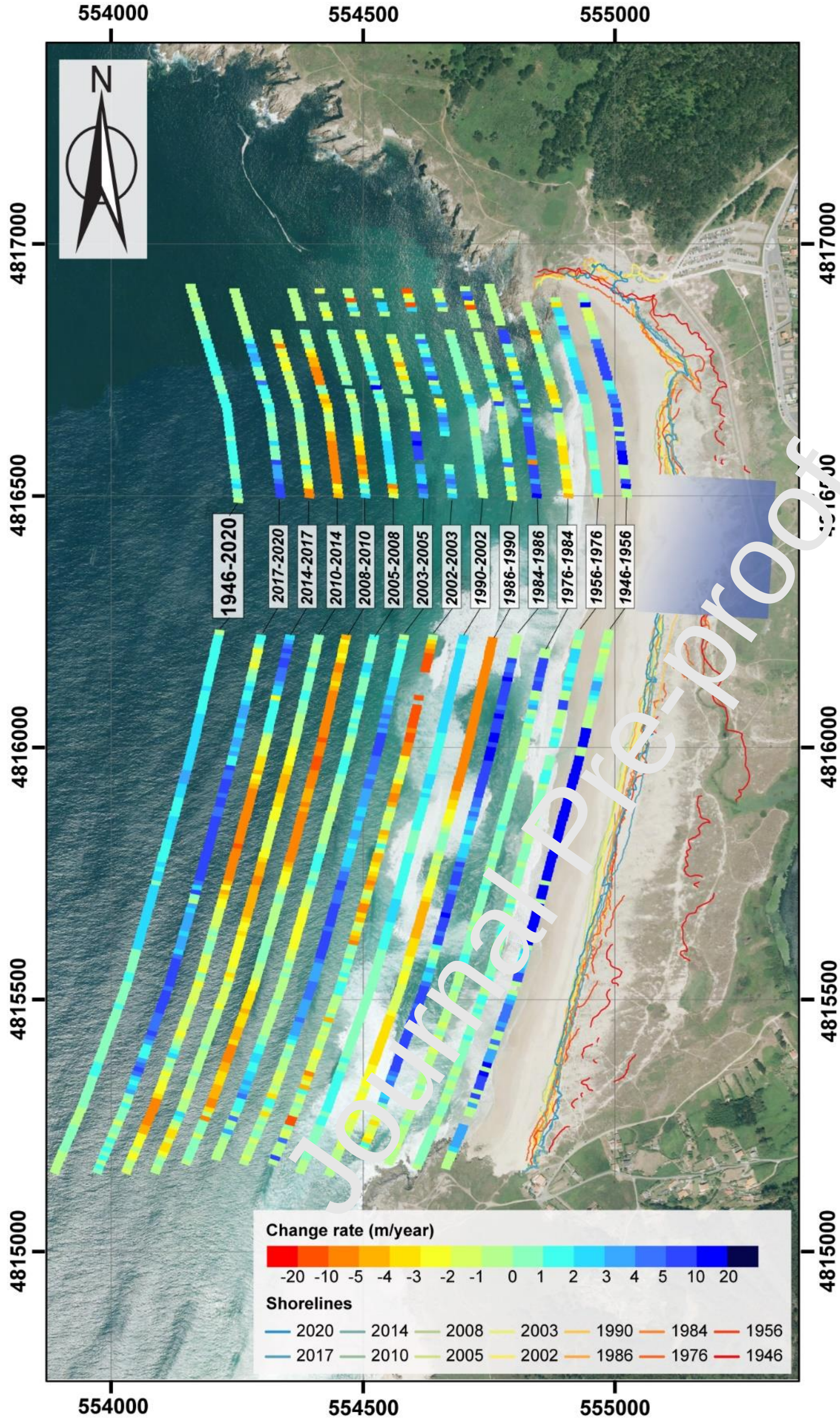

Figure 3. Rate of shoreline change on the Doniños coast over 1945-2020 is delineated by the colored bands; seaward advance (accretion) and landward retreat (erosion) of the shoreline is shown in red and blue, respectively. The thin, continuous lines denote the shoreline position on each available date, and the blue shaded area was omitted fromthe analysis.

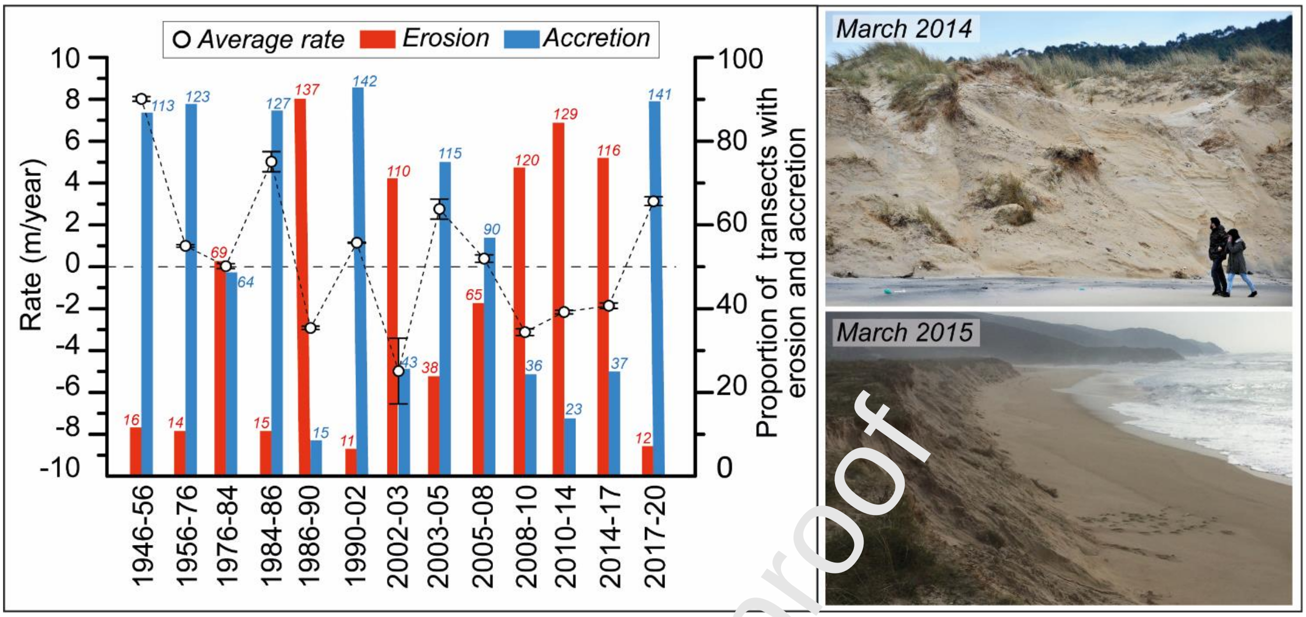

Figure 4. The proportions of the shoreline that have experienced erosion (red bars) and accretion (blue bars) during the periods with available data. The numbers above the bars indicate the number of transects with negative or positive distances, and the white dots correspond to the average rate and standard deviation (in m/year) in each analyzed period. The photographs on the right are examples of dune scarps in March 2014* and March 2015 following extreme wave events (*source: La Voz de Galicia, author Ángel Manso).

The topographic profiles of 2010 show the pre-erosion state before the storm event in 2015 (Figures 4 and 5A), and the 2019 profiles (coincident with the GPR sampling year) show an initial shoreline recovery process observed in the shoreline analysis between 2017 and 2020 (Figures 3 and 4). This was reflected in the internal architecture of the foredune in the GPR profiles, which showed a final recovery phase of the foredune toe from 2017 to 2019 (Figure 5B).

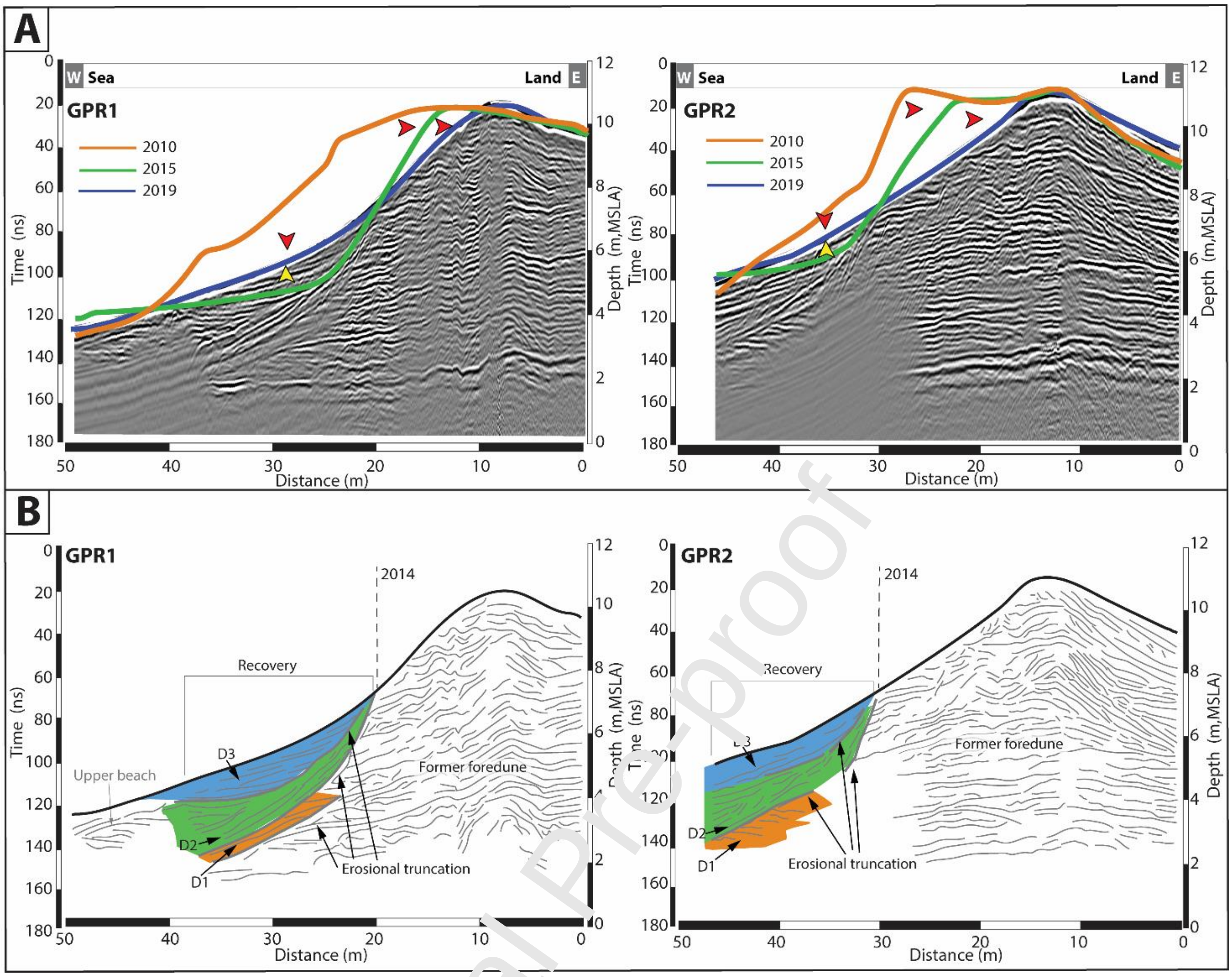

Figure 5. (A) GPR-derived 200-MHz antenna radargrams and topographic profiles obtained from the DEMs data in 2010 and 2015 and DGPS surveys in 2019 on the foredune of the Doniños barrier considering the chronological framework constrained by the aerial imagery and topographic data interpretation. The red arrows indicate a retreating and lowering foredune, while the yellow arrows denote the upper beach and foredune accretion. (B) GPR data interpretation; the radar units define the internal architecture and structure of the foredune recovery (units D1 to D3), and the inferred position of the shoreline in 2014 (dashed line).

Three of the radar units defined the onset of foredune recovery (D1 to D3, Figure 7B). Unit D1 (orange) displayed sigmoidal or oblique reflectors that defined incipient foredune growth, which was interpreted as an accretional phase on the former foredune. Unit D2 (green) overlaid unit D1 and was characterized by a seaward-dipping reflection configuration with a downlap reflector termination on the upper D1 boundary, and unit D3 (blue) overlaid unit D2 and was defined by a seaward-dipping reflection with a downlap reflector termination on the D2 unit boundary. Subparallel reflections characterized the upper-subaerial beach in the GPR1 radargram. The topographic profiles corresponding to 2010 (orange) and 2015 (green) showed that an erosive episode occurred during this period and was characterized by the lowering of the topographic profile and the retreat of the foredune crest (Figure 7A), and the trace of the 2015 profile was coincident with the landward limit of the erosional truncation between units D2 and D3. Because the 2014 shoreline (dashed line in Figure 5B), represented the seaward limit of the foredune and was coincident with the landward position of the erosional truncation between unit D2 and the former foredune, this erosional truncation was though to possibly originate from storms that occurred in 2014, and D2 could be attributed to the recovery between 2014 and 2015. The timing of the D1 cannot be attributed to a specific date within the available data, but it reflected a possible depositional event at a different earlier period.

4.2 Coastal dune vegetation cover changes

The dune showed an overall increase in vegetation cover between 1945 and 2020 (Figure 6), despite some periods of decreasing vegetation cover. In 1945, the dune was sparsely vegetated, with a vegetation cover of 15.1% (Figure 6). From 1945 to 1976, the vegetation gradually spread until it covered approximately 61% of the total area. The vegetation cover decreased by 13% during 1976-1984, coincident with the slight shoreline erosion observed in the same time window (Figure 7). The vegetation recovered in the following years, reaching a 71% coverage by 1986, which was higher than that in 1976 (Figure 6). This vegetation expansion coincided with the shoreline accretion observed during the same period (Figure 7). Between 1980 and 1990, the vegetation cover decreased to below 65% (Figure 6), while the shoreline retreated (Figure 7). After that, the vegetation cover reached its maximum extent in 2008 (78.3%). Thereafter, the vegetation coverage decreased to 65.6% in 2017 (Figure 6), which coincided with the observed progressive retreat of the shoreline (Figure 7).

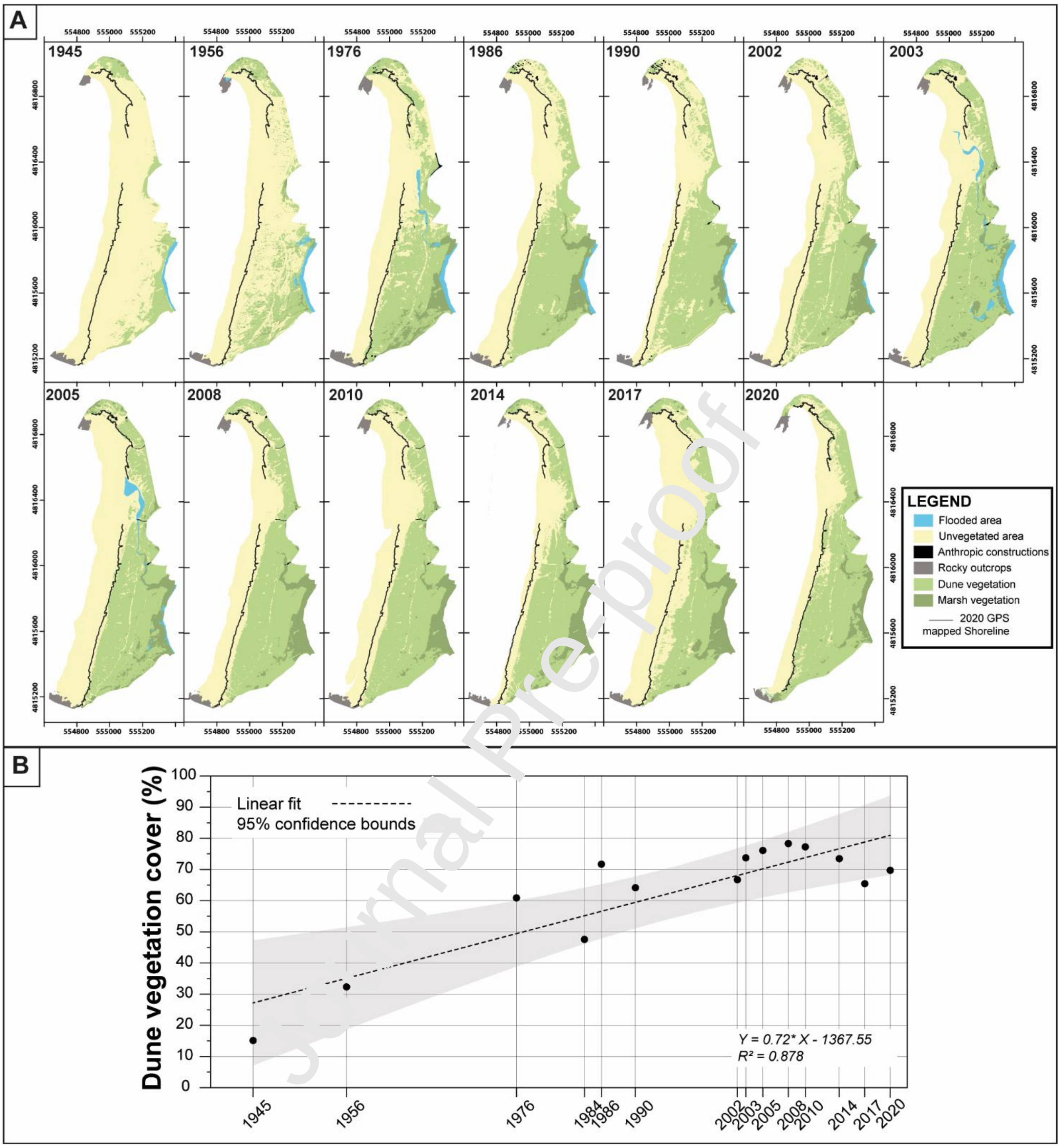

Figure 6. A: Map series showing changes in the surficial units of the Doniños coastal system from 1945 to 2017. The solid black line corresponds to the limit between the vegetated dunes and the sandy beach, as mapped in 2020 with a GPS-RTK and which are plotted as references in all the maps. B. Black dots represent the vegetation cover values (in percentages) over the study period, with the trend line and 95% confidence limits

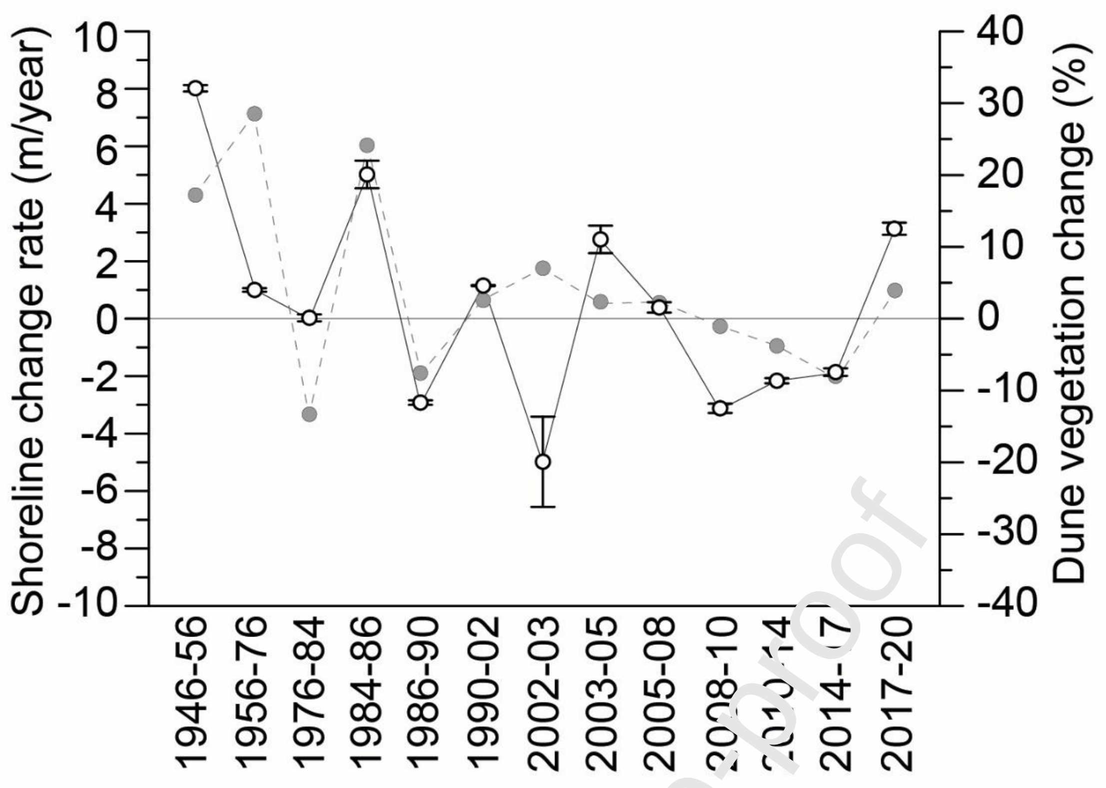

Figure 7. Chart showing shoreline change rate in m/year (white circles) and vegetation cover percentage changes (gray circles) over the evaluated period. See the text for a more detailed explanation.

4.3 Changes in wind and wave conditions

The onshore wave conditions from 1958 to 2020 showed strong seasonality, with energetic waves (generally exceeding $H_{s95\%}$) occurring during the winter, and much weaker conditions (generally lower than $H_{s95\%}$) occurring during the summer (Figure 8A). Storm wave conditions occurred during the winter and summer seasons (Figure 8B). However, storm clusters mainly occurred during the winter season. Furthermore, the storm intensity, in terms of duration, the storm frequency, and the number of observations (Figure 8B), were also greater in winter than in summer. The periods of more frequent storm clusters occurred before the 1980s, and in the last part of the record, i.e., after 2013. In contrast, isolated winter storms were more frequent between 1980 and 2010.

The onshore wave power distribution and its longshore and cross-shore components showed a clear seasonal pattern, with increasingly variable values during the winter season (Figure 8C). The three variables followed a similar pattern, with a higher interannual variability of onshore wave power and its longshore component, despite the apparent concentration of wave energy around 1959, 1972, 1982, 1984, 1986, 2014, and 2018-2019, with the highest values occurring in 2014.

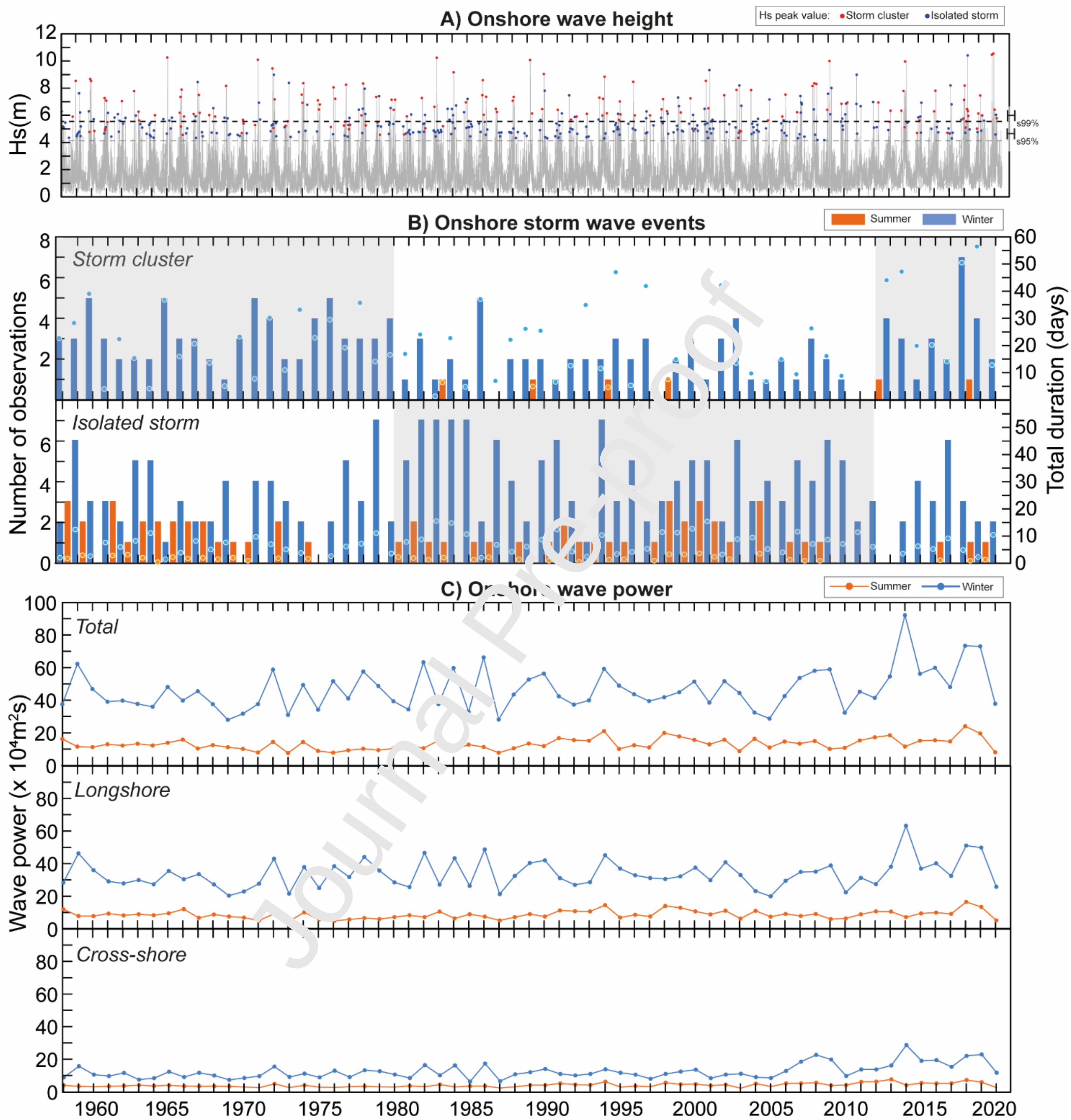

Figure 8: Time series of onshore-directed waves extracted from the SIMAR-3028036 node (see location in Figure 1), wave energy density, wave power and number and duration of storm waves. (A) The significant wave height (solid gray line), $H_{s95\%}$ and $Hs_{99\%}$ (dashed lines) were calculated over the entire period. The circles correspondto the peak Hs values during storm clusters (red circles) and isolated storms (blue circles). (B) Number of observations if identified storm clusters and isolated storms in winter (light blue bars) and summer (orange bars). Duration (in days) of storm clusters and isolated storms in the winter (light blue dots) and summer (orange dots) seasons. Gray shaded areas indicate the periods in which

clusters or isolated storms were dominant. (C) Total wave power, longshore and cross-shore components for the winter (light blue solid lines) and summer (orange solid line) seasons.

The only wind directions with a significant impact on the Doniños dune field range from 190° (SSW) to 10° (NNE). Three distinctive wind regime periods were identified according to their duration (in hours) and annual potential sediment transport (Figures 9A and 9B). Period 1 (P1), which occurred between 1931 and 1955, was characterized by a higher occurrence of winds above the sand transport threshold velocity, whose events totalled more hours during winter than during summer (Figure 9A). Period 2 (P2), from 1955 to 1990, had a reduction in onshore potential transport and the total duration (in hours) of events exceeding the transport threshold; this reduction was more pronounced in the summer season. Period 3 (P3) occurred after 1990 and was characterized by the lowest values of potential sediment transport, a narrower variability and lower peak values, with notably fewer hours of winds that exceed the sand transport threshold.

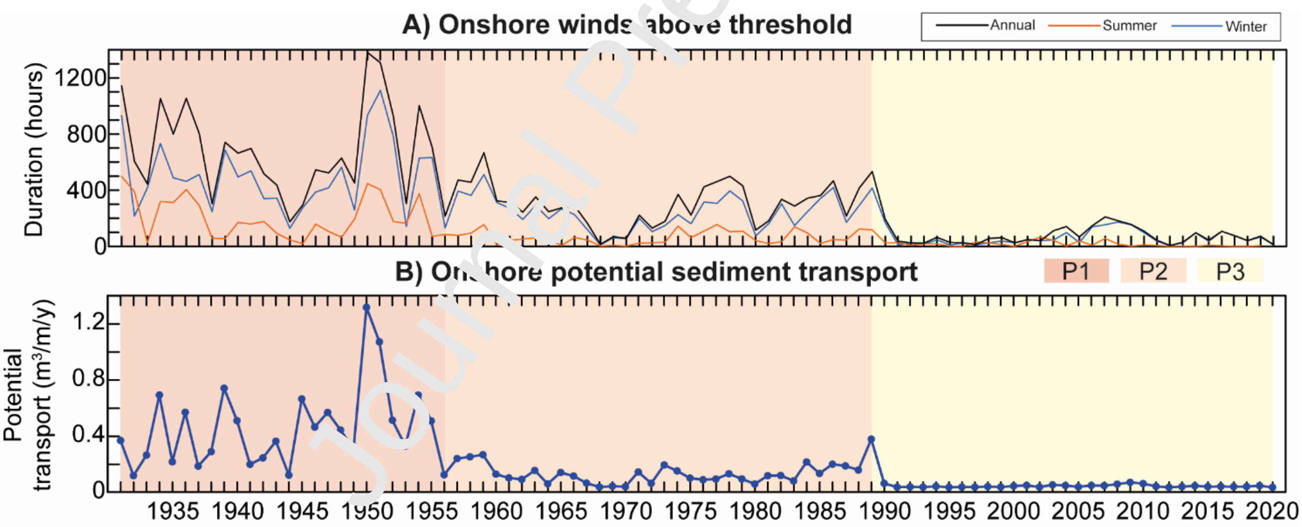

Figure 9. (A) Total seasonal and annual hours during which aeolian events exceeded the sand transport threshold (B) Annual sediment transport potential generated by onshore winds that exceeded the sand transport threshold of 7.48 m/s , calculated using the Bagnold (1936) equations (see Methods). The three distintcive periods of P1 to P3 are indicated by shadded areas of different colors

5. DISCUSSION

5.1 Role of primary drivers on decadal coastal dune variabilities

Over the last 70 years, the evolution of the Doniños dune has been characterized by net seaward shoreline advance and an increase in vegetation. However, both changes were neither gradual nor linear during the analyzed time period (1946-2020). The changes in the shoreline location and the dune vegetation seaward boundary were closely interrelated (Figure 7) and were ultimately driven by the recurrence of onshore-directed storm wave events. During these events the extreme wave water level exceeded the $H_{s99\%}$ value (in this case 5.55 m), and the values were almost certainly higher due to wave run-up. Considering, that the dune foot in Doniños could be set between 4.5-5 m (Figure 5), the impact of these storm events predictably provoked the erosion of the foredune and the destruction of its vegetation, as observed elsewhere (Carter, 1990; Hesp, 2002; Houser et al., 2018). This process was clearly recognized in the Doniños system from 2008 to 2017 and coincided with the change in the storm pattern (Figure 8) against a backdrop of sea level rise (Masselink et al., 2016; Vousdoukas et al., 2017). During this period, increased recurrences of wave storm cluster events were observed alongside strong onshore wave power, and extreme storm surges reached their maximum in 2013/14 (Figures 4 and 8). Therefore, the maximum erosion was recorded between 2010 and 2014 and was manifested as a 90% retreat of the dune-extension region (Figure 4). This was also clearly identifiable in the topographic profiles extracted from the DEMs and GPR data (Figure 5). It is worthy to highlight, that this episode was not a consequence of local climate instability, but rather coincided with an extraordinary series of high-energy storms that affected western Europe and caused severe erosion along sandy (Diogo et al., 2014; Dodet et al., 2019; Flor et al., 2015; Héquette et al., 2019; Masselink et al., 2016; Santos et al., 2014) and rocky coasts (Cox et al., 2018; Gómez-Pazo et al., 2019; Oliveira et al., 2020).

After the winter of 2013/14, the recovery of the eroded foredune was not spatiotemporally constant, likely due to the recurrent impacts of winter storm surges in successive years (such as the storm events observed in 1990-2002 and 2003-2005, Figures 4 and 8), which affected the usual dune recovery process. Moreover, this recovery might have been hindered by the decreased transport of sufficient sand from the beach to the dune due to the weakening of the onshore winds the following summers (Figure 9). This was seen in the GPR profiles, with the 2019 foredune profile still exhibiting a landward position similar to that in 2010 (Figure 5A). These findings demonstrate that after 2008, wave-induced processes were the dominant primary factors forcing foredune erosion and vegetation loss.

The dune vegetation cover resembled the evolution documented in the nearby Traba coastal dune field (see location in Figure 1), where an increase in the vegetation cover was documented over the same period (1940-2008) and was found to be related to a reduction in the wind intensity (González-Villanueva et al., 2013). Both cases also support the observed worldwide greening of coastal dunes (Jackson et al., 2019), as greening makes dunes more resistant to extreme marine events. Likewise, our findings agree with the global wind stilling hypothesis proposed by several authors (McVicar et al., 2012; Vautard et al., 2010; Zhang et al., 2019), despite the revived debate suggesting a trend reversal, wind recovery and dune reactivation since 2010 (Gao et al., 2022; Wohland et al., 2021; Zeng et al., 2019). No evidence of this reversal trend was detected in the Doniños system after 2010 (Figure 9).

5.2 A conceptual model of the Doniños dune evolution process over the last 70 years

The main emergent idea of this work was that a subtle and unbalanced interplay existed between wind stilling and the frequency and/or intensity of storm surges associated with energetic winters; we think that this interplay can explain the decadal coastal dune landscape changes that were observed in the Doniños system (Figure 10). The progressive expansion of this dune system was directly related to the overall wind stilling over recent decades (Figure 10, stages A and B), which made the dune more resistant to erosion. Conversely, energetic winters could prompt vegetation coverage deterioration due to foredune retraction and the subsequent vegetation burial associated with the seasonal aeolian accumulation of sand (Figure 10, stage C1). When wind stilling conditions persisted during the subsequent summer, a reduction in the sediment supply to the foredune occurred. This reduction likely resulted in further hindrance of the foredune recovery, making it more vulnerable to marine erosion and diminishing its resistance (Figure 10, stage D1). Alternatively, if the wind held sufficient energy to exceed the grain threshold capacity required for sand transport the following summer, thus allowing the entrainment of sand on the beach and its subsequent transport to the dune, the foredune could quickly recover, counteracting the potential erosion that may have occurred the following winter (Figure 10, stage D2). On the other hand, mild winters result in low levels or no foredune erosion (Figure 10, stage C2) from which the foredune can easily recover the following summer (Figure 10, stage E1) or even experience a net increase if sufficient wind energy is present (Figure 10, stage E2). Consequently, foredune evolution is primarily driven by the recurrence or absence of energetic winters, as they can reverse or stall foredune recovery.

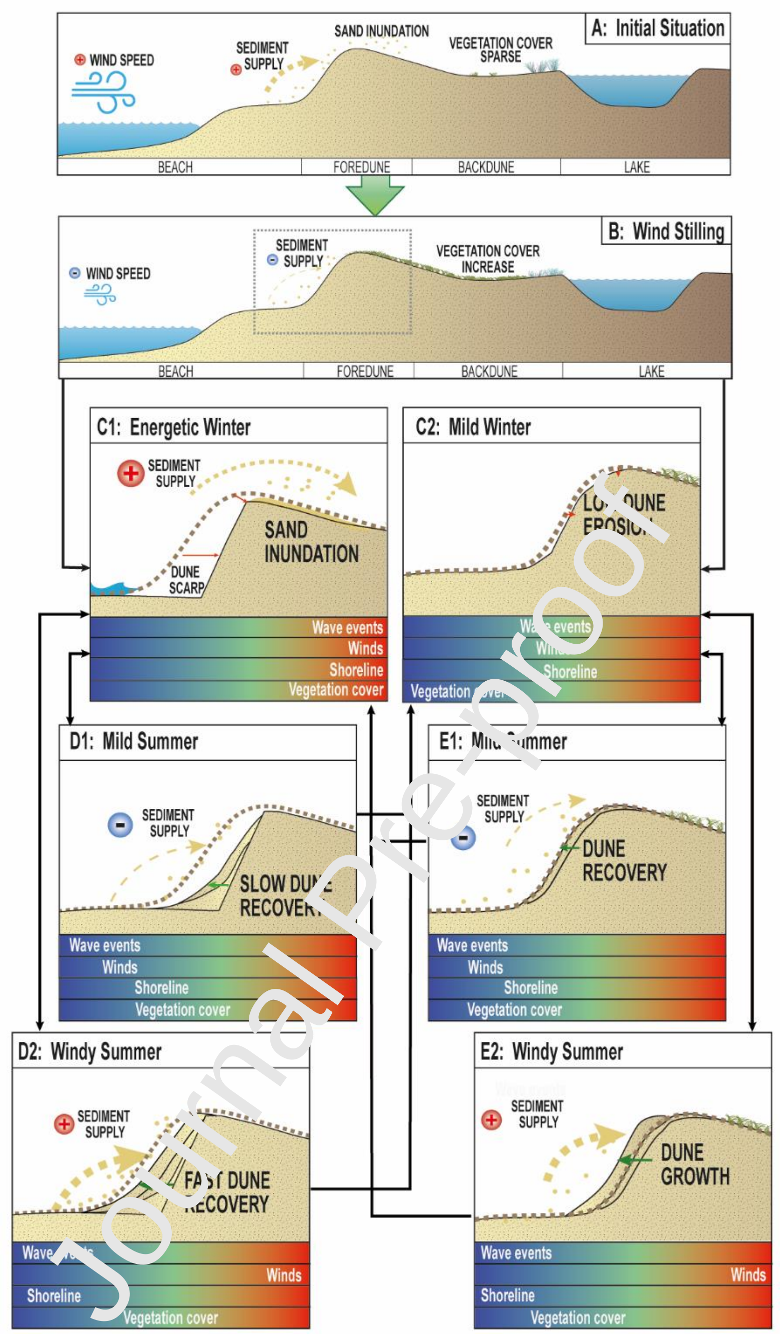

Figure 10. Conceptual model of the evolutionary behavior of the Doniños coastal dune system since the mid-20th century. The conceptual model includes four behavior stages, from the initial situation (A) of the active, unvegetated dune to the wind stilling conditions that may have increased the stability of the dune system and the vegetation cover expansion period (B) following the plausible evolution of the foredune area, shoreline position and vegetation cover, which are dependent on climatic conditions over consecutive winters (C1 and C2) and summers (D1-D2 and E1-E2). In the color maps in panels C to E, blue indicates the lowest wind and wave conditions, which are associated with increasing vegetation cover and an advancing shoreline position, and red indicates strong wind and storm wave conditions, which

correspond to decreasing vegetation cover and shoreline retreat. See the text for a more in-depth explanation of these processes.

5.3 Implications and future perspectives

Currently, vegetated dunes critically protect large coastal stretches from marine flooding. Considering current sea-level rise, the pressures placed on these systems are expected to increase (Leatherman et al., 2000). These pressures will also be accentuated in most coastal embayment systems where the accommodation space is constrained by bedrock topographic morphologies or artificial barriers that restrain natural landward marine migration spurred by sea-level rise, such as that observed in the Doniños coastal system. In this context, dune vegetation plays a crucial role in coastal landscape evolution; it entraps the sand that is transported by wind, thus controlling the shape and height of the dune (Durán and Moore, 2013). In turn, the presence of dune vegetation makes the dune more resistant to storm waves and diminishes the erosion impacts of subsequent storms until the wave energy surpasses a certain threshold. Under these circumstances, destabilization will induce a regression to the characteristic landscape developed during the 1940s, and significant shoreline retreat. In contrast, recurring and/or increasingly intense storm surges will have the undesired effect of significantly reducing the extension of coastal dune habitats due to the combined effect of shoreline retreat and the lack of sufficient landward accommodation space. Therefore, if persistent storm surges, similar to those observed from 2008 to 2017, recur in the near future, the system will face an important spatial regression.

Additional climatic and geomorphological studies are needed to develop a complete regional picture of the response to future climate change scenarios. These studies should consider the role of atmospheric circulation patterns and their future changes and impacts over the Iberian Atlantic Margin. Regionally recurrent atmospheric variability patterns, such as the North Atlantic Oscillation (NAO) and the East Atlantic (EA) and Scandinavia (SCA) patterns, are known to modulate meteorological variables, which are primary drivers of coastal changes (González-Villanueva et al., 2013; Hernández et al., 2015; Hurrell, 1995; Martínez-Asensio et al., 2016; Trigo et al., 2008). In fact, previous studies have stressed the effects of these atmospheric variability patterns over the metocean climate, particularly those of the NAO index in winter (Costas and Alejo, 2007; Dodet et al., 2010; Lebreiro et al., 2006; Pye and Blott, 2008) and the EA index in summer (deCastro et al., 2008; González-Villanueva et al., 2013; Hernández et al., 2021). However, the NAO index failed to explain the high wave energy levels observed during the winter of 2013/14, and a new index, the West Pressure Anomaly (WEPA) was designed to represent the wave climate on the European Atlantic coast (Castelle et al., 2017). The winter-averaged WEPA had the most robust relationship with the interannual metocean dynamics along the Atlantic Iberian coast (Castelle et al., 2017; Villacieros-Robineau et al., 2021). Therefore, further research should be conducted to investigate the roles that all these patterns play in regional extreme events and their impacts on coastal (eco)systems.

6. CONCLUSIONS

Since the middle of the 20th century, the sandy Doniños coastal dune system has experienced net seaward shoreline advance and vegetation cover expansion; the latter was likely triggered by the wind stilling that was reported for the NW coast of Spain since the end of the 1950s.

The changes in the vegetation cover and shoreline position were interrelated during recent decades due to the shifting dynamics of the foredune area. The wave-induced processes dominated wind impacts as the main factors forcing foredune erosion and vegetation loss, therefore affecting the evolution of the dune landscape.

The stalling or reversal of foredune advance through erosion is dependent on the overall frequency and magnitude of energetic winters.

A conceptual model was proposed to explain the relationship between foredunes and instability climate changes. Briefly, this model states that coastal dune landscape evolution is determined, at a decadal temporal scale, by the uneven interplay between wind stilling and the frequency and/or intensity of storm surges that are associated with energetic winters.

This research provides additional evidence supporting the global wind stilling hypothesis. The results, however, point to a particular dichotomy and imbalance in the effects of wind stilling. Wind weakening increased the resistance of the studied dune to the impacts of marine erosion by expanding the dune vegetation, but paradoxically, it could also reduce the recovery capacity of the foredune profile after an energetic winter by reducing the wind capacity that is responsible for transferring sand from the beach to the dune.

The interrelations between coastal dunes, wind and waves shown in the conceptual model, are very useful for understanding the coastal landscape evolution of coastal zones that are similar to the Galician coast. In addition, they can help to clarify the negative consequences of a variable wave and wind regime, including shoreline retreat and vegetation cover decay, or the positive consequences, which is beneficial for coastal management purposes.

ACKNOWLEDGMENTS

This work was supported by the PALEOMODES (CGL2016-75281-C2) and IMPACOM (PID2019-107424RB-I00) projects of the Spanish Ministry of Economy and Competitiveness and the Ministry of Science and Innovation, respectively. The authors also thank Puertos del Estado for providing SIMAR point data and the Agencia Estatal de Meteorología (AEMET) for providing climate data. AH is funded by the Spanish Ministry of Science and Innovation through the Ramón y Cajal Scheme (RYC2020-029253-I). This work is a contribution to IGCP Project 725 'Forecasting Coastal Change'. Funding for open access charge was provided by the Universidade de Vigo/CISUG.

REFERENCES

Anderson, T.R., Frazer, L.N., Fletcher, C.H., 2014. Long-Term Shoreline Change at Kailua, Hawaii, Using Regularized Single Transect. Journal of Coastal Research 31, 464–476. https://doi.org/10.2112/JCOASTRES-D-13-00202.1

Arkema, K.K., Guannel, G., Verutes, G., Wood, S.A., Guerry, A., Ruckelshaus, M., Kareiva, P., Lacayo, M., Silver, J.M., 2013. Coastal habitats shield people and property from sea-level rise and storms. Nature Climate Change 3, 913–918. https://doi.org/10.1038/nclimate1944

Bagnold, R.A., 1941. The Physiscs of Blown Sand and Deserts Dunes, Morrow, New York.

Bagnold, R.A., 1936. The movement of desert sand. Proceedings of the Royal Society of London 157, 594–620. https://doi.org/10.1098/rspa.1936.0218

Barbier, E.B., Hacker, S.D., Kennedy, C., Koch, E.W., Stier, A.C., Silliman, B.R., 2011. The value of estuarine and coastal ecosystem services 81, 169–193. https://doi.org/10.1890/10-1510.1

Boak, E.H., Turner, I.L., 2005. Shoreline Definition and Detection: A Review. Journal of Coastal Research 2005, 688–703. https://doi.org/10.2112/03-0071.1

Bristow, C.S., Bailey, S.D., Lancaster, N., 2000. The sedimentary structure of linear sand dunes. Nature 406, 56–59.

Carter, R.W.G., 1990. The geomorphological, ecological and pedological development of coastal foredunes at Magilligan Point, Northern Ireland, in: K.F. Nordstrom, N.P.P., Carter, R.W.G. (Eds.), . Wiley, Chichester, p. 129.

Castelle, B., Dodet, G., Masselink, G., Scott, T., 2017. A new climate index controlling winter wave activity along the Atlantic coast of Europe: The West Europe Pressure Anomaly. Geophysical Research Letters 44, 1384–1392. https://doi.org/10.1002/2016GL072379

Castelle, B., Guillot, B., Marieu, V., Chaumillon, E., Hanquiez, V., Bujan, S., Poppeschi, C., 2018. Spatial and temporal patterns of shoreline change of a 280-km high-energy disrupted sandy coast from 1950 to 2014: SW France. Estuarine, Coastal and Shelf Science 200, 212–223. https://doi.org/10.1016/j.ecss.2017.11.005

Castelle, B., Marieu, V., Bujan, S., Splinter, K.D., Robinet, A., Sénéchal, N., Ferreira, S., 2015. Impact of the winter 2013–2014 series of severe Western Europe storms on a double-barred sandy coast: Beach and dune erosion and megacusp embayments. Geomorphology 238, 135–148. https://doi.org/10.1016/j.geomorph.2015.03.006

Castelle, B., Ritz, A., Marieu, V., Nicolae Lerma, A., Vandenhove, M., 2022. Primary drivers of multidecadal spatial and temporal patterns of shoreline change derived from optical satellite imagery. Geomorphology 413, 108360. https://doi.org/10.1016/j.geomorph.2022.108360

Costa, P.J.M., Costas, S., González-Villanueva, R., Oliveira, M.A., Roelvink, D., Andrade, C., Freitas, M.C., Cunha, P.P., Martins, A., Buylaert, J.P., Murray, A., 2016. How did the AD 1755 tsunami impact on sand barriers across the southern coast of Portugal? Geomorphology 268, 296–311. http://dx.doi.org/10.1016/j.geomorph.2016.06.019

Costas, S., Alejo, I., 2007. Local and global influences on the evolution of a transgressive sand barrier: Cíes Barrier, Northwest Spain. Journal of Coastal Research SI50, 1121–1125.

Costas, S., Alejo, I., Rial, F., Lorenzo, H., Nombela, M.A., 2006. Cyclical evolution of a modern transgressive sand barrier in NW-Spain elucidated by GPR and aerial photo. Journal of Sedimentary Research 76, 1077–1092.

Cox, R., Jahn, K.L., Watkins, O.G., Cox, P., 2018. Extraordinary boulder transport by storm waves (west of Ireland, winter 2013–2014), and criteria for analysing coastal boulder deposits. Earth-Science Reviews 177, 623–636. https://doi.org/10.1016/j.earscirev.2017.12.014

deCastro, M., Gómez-Gesteira, M., Lorenzo, M.N., Alvarez, I., Crespo, A.J.C., 2008. Influence of atmospheric modes on coastal upwelling along the western coast of the Iberian Peninsula, 1985 to 2005. Climate Research 36, 169–179.

Diogo, Z., Bastos, A., Ponte Lira, C., Taborda, R., Andrade, C.F., Silveira, T., Ribeiro, M., Silva, A., Carapuço, M., Aleixo Pinto, C., Freitas, M., 2014. Morphological impacts of Christina storm on the beaches of the central western Portuguese coast 101, 1445–1448.

Dodet, G., Bertin, X., Taborda, R., 2010. Wave climate variability in the North-East Atlantic Ocean over the last six decades. Ocean Modelling 31, 120–131. https://doi.org/10.1016/j.ocemod.2009.10.010

Dodet, G., Castelle, B., Masselink, G., Scott, T., Davidson, M., Floc'h, F., Jackson, D., Suanez, S., 2019. Beach recovery from extreme storm activity during the 2013–14 winter along the Atlantic coast of Europe. Earth Surface Processes and Landforms 44, 393–401. https://doi.org/10.1002/esp.4500

Durán, O., Moore, L.J., 2013. Vegetation controls on the maximum size of coastal dunes. Proceedings of the National Academy of Sciences 110, 17217–17222. https://doi.org/10.1073/pnas.1307580110

EEA, 2006. The changing faces of Europe's coastal areas. European Environmental Agency, Copenhagen.

Flor, G., Flor-Blanco, G., Soriano, C.F.-, 2015. Cambios ambientales por los temporales de invierno de 2014 en la costa asturiana (NO de España). Trabajos de Geología 34, 97–123. https://doi.org/10.17811/tdg.34.2014.97-123

Fortunato, A.B., Meredith, E.P., Rodrigues, M., Freire, P., Feldmann, H., 2019. Near-future changes in storm surges along the Atlantic Iberian coast. Natural Hazards 98, 1003–1020. https://doi.org/10.1007/s11069-018-3375-z

Gao, J., Kennedy, D.M., Konlechner, T.M., McSweeney, S., Chiaradia, A., McGuirk, M., 2022. Changes in the vegetation cover of transgressive dune fields: A case study in Cape Woolamai, Victoria. Earth Surface Processes and Landforms 47, 778–792. https://doi.org/10.1002/esp.5284

Girardi, J.D., Davis, D.M., 2010. Parabolic dune reactivation and migration at Napeague, NY, USA: Insights from aerial and GPR imagery. Geomorphology 114, 530–541. https://doi.org/10.1016/j.geomorph.2009.08.011

Gómez-Pazo, A., Pérez-Alberti, A., Trenhaile, A., 2019. Recording inter-annual changes on a boulder beach in Galicia, NW Spain using an unmanned aerial vehicle. Earth Surface Processes and Landforms 44, 1004–1014. https://doi.org/10.1002/esp.4549

González-Villanueva, R., Costas, S., Pérez-Arlucea, M., Jerez, S., Trigo, R.M., 2013. Impact of atmospheric circulation patterns on coastal dune dynamics, NW Spain. Geomorphology 185, 96–109. http://dx.doi.org/10.1016/j.geomorph.2012.12.019

González-Villanueva, R., Pérez-Arlucea, M., Costas, S., 2017. Lagoon water-level oscillations driven by rainfall and wave climate. Coastal Engineering 130, 34–45. https://doi.org/10.1016/j.coastaleng.2017.09.013

Héquette, A., Ruz, M.-H., Zemmour, A., Marin, D., Cartier, A., Sipka, V., 2019. Alongshore Variability in Coastal Dune Erosion and Post-Storm Recovery, Northern Coast of France. Journal of Coastal Research 88, 25–45. https://doi.org/10.2112/SI88-004.1

Hernández, A., Cachão, M., Sousa, P., Trigo, R.M., Luterbacher, J. ürg, Vaquero, J.M., Freitas, M.C., 2021. External forcing mechanisms controlling the North Atlantic coastal upwelling regime during the mid-Holocene. Geology 49, 433–437. https://doi.org/10.1130/G48112.1 %J Geology

Hernández, A., Trigo, R.M., Pla-Rabes, S., Valero-Garcés, B.L., Jerez, S., Rico-Herrero, M., Vega, J.C., Jambrina-Enríquez, M., Giralt, S., 2015. Sensitivity of two Iberian lakes to North Atlantic atmospheric circulation modes. Climate Dynamics 45, 3403–3417. https://doi.org/10.1007/s00382-015-2547-8

Herrero, X., Costas, S., Kombiadou, K., 2020. Coastal ridge constructive processes at a multi-decadal scale in Barreta Island (southern Portugal). Earth Surface Processes and Landforms 45, 411–423. https://doi.org/10.1002/esp.4742

Hesp, P., 2002. Foredunes and blowouts: initiation, geomorphology and dynamics. Geomorphology 48, 245–268. https://doi.org/10.1016/s0169-555x(02)00184-8

Himmelstoss, E.A., Henderson, R.E., Kratzmann, M.G., Farris, A.S., 2018. Digital Shoreline Analysis System (DSAS) version 5.0 user guide. https://doi.org/10.3133/ofr20181179

Houser, C., Figlus, J., Hammond, B., 2018. Post-storm recovery of the foredune: Implications for barrier island resiliency. Presented at the AGU Fall Meeting Abstracts, pp. EP23C-2346.

Hurrell, J.W., 1995. Decadal Trends in the North Atlantic Oscillation: Regional Temperatures and Precipitation. Science 269, 676–679. https://doi.org/10.1126/science.269.5224.676

Jackson, D.W.T., Costas, S., González-Villanueva, R., Cooper, A., 2019. A global 'greening' of coastal dunes: An integrated consequence of climate change? Global and Planetary Change 182, 103026. https://doi.org/10.1016/j.gloplacha.2019.103026

Kirezci, E., Young, I.R., Ranasinghe, R., Muis, S., Nicholls, R.J., Lincke, D., Hinkel, J., 2020. Projections of global-scale extreme sea levels and resulting episodic coastal flooding over the 21st Century. Scientific Reports 10, 11629. https://doi.org/10.1038/s41598-020-67736-6

Komar, P.D., 1976. Beach processes and sedimentation. Prentice-Hall, Inc, Engewood Cliffs, New Jersey.

Leatherman, S.P., Zhang, K., Douglas, B.C., 2000. Sea level rise shown to drive coastal erosion. Eos Archives 81, 55–57. https://doi.org/10.1029/00EO00034

Lebreiro, S.M., Francés, G., Abrantes, F.F.G., Diz, P., Bartels-Jónsdóttir, H.B., Stroynowski, Z.N., Gil, I.M., Pena, L.D., Rodrigues, T., Jones, P.D., Nombela, M.A., Alejo, I., Briffa, K.R., Harris, I., Grimalt, J.O., 2006. Climate change and coastal hydrographic response along the Atlantic Iberian margin (Tagus Prodelta and Muros Ría) during the last two millennia. The Holocene 16, 1003–1015. https://doi.org/10.1177/0959683606hl990rp

Lorente, P., Sotillo, M.G., Aouf, L., Amo-Baladrón, A., Barrera, E., Dalphinet, A., Toledano, C., Rainaud, R., Alfonso, M.D., Piedracoba, S., Basañez, A., García-Valdecasas, J.M., Pérez-Muñuzuri, V., Álvarez-Fanjul, E., 2018. Extreme Wave Height Events in NW Spain: A Combined Multi-Sensor and Model Approach. Remote Sensing 10, 1.

Martínez-Asensio, A., Tsimplis, M.N., Marcos, M., Feng, X., Gomis, D., Jordà, G., Josey, S.A., 2016. Response of the North Atlantic wave climate to atmospheric modes of variability. International Journal of Climatology 36, 1210–1225. https://doi.org/10.1002/joc.4415

Masselink, G., Austin, M., Scott, T., Poate, T., Russell, P., 2014. Role of wave forcing, storms and NAO in outer bar dynamics on a high-energy, macro-tidal beach. Geomorphology 226, 76–93. https://doi.org/10.1016/j.geomorph.2014.07.025

Masselink, G., Castelle, B., Scott, T., Dodet, G., Suanez, S., Jackson, D., Floc'h, F., 2016. Extreme wave activity during 2013/2014 winter and morphological impacts along the Atlantic coast of Europe. Geophysical Research Letters 43, 2135–2143. https://doi.org/10.1002/2015GL067492

McCormick, ME., Kraemer, DRB., 2001. Wave Energy, in: Encyclopedia of Ocean Sciences. Elsevier, Amsterdam.

McVicar, T.R., Roderick, M.L., Donohue, R.J., Niel, T.G.V., 2012. Less bluster ahead? Ecohydrological implications of global trends of terrestrial near-surface wind speeds. Ecohydrology 5, 381–388. https://doi.org/10.1002/eco.1298

Murray, A.B., Knaapen, M.A.F., Tal, M., Kirwan, M.L., 2008. Biomorphodynamics: Physical-biological feedbacks that shape landscapes. Water Resources Research 44. https://doi.org/10.1029/2007WR006410

Neal, A., 2004. Ground-penetrating radar and its use in sedimentology: principles, problems and progress. Earth-Sci. Rev. 66, 261–330. https://doi.org/10.1016/j.earscirev.2004.01.004

Oliveira, M.A., Scotto, M.G., Barbosa, S., Andrade, C.F. de, Freitas, M. da C., 2020. Morphological controls and statistical modelling of boulder transport by extreme storms. Marine Geology 426, 106216. https://doi.org/10.1016/j.margeo.2020.106216

Oppenheimer, M., Glavovic, B.C., Hinkel, J., Wal, R., Magnan, A.K., Abd-Elgawad, A., Cai, R., Cifuentes-Jara, M., DeConto, R.M., Ghosh, T., Hay, J., Isla, F., Marzeion, B., Meyssignac, B., Sebesvari, Z., 2019. IPCC SR Chapter 4: Sea Level Rise and Implications for Low-Lying Islands, Coasts and Communities.

Pye, K., Blott, S.J., 2008. Decadal-scale variation in dune erosion and accretion rates: An investigation of the significance of changing storm tide frequency and magnitude on the Sefton coast, UK. Geomorphology 102, 652–666. https://doi.org/10.1016/j.geomorph.2008.06.011

Reynolds, J.M., 1997. An Introduction to Applied and Environmental Geophysics. John Wiley, New York, USA.

Robin, N., Billy, J., Castelle, B., Hesp, P., Lerma, A.N., Laporte-Fauret, Q., Marieu, V., Rosebery, D., Bujan, S., Destribats, B., Michalet, R., 2021. 150 years of foredune initiation and evolution driven by human and natural processes. Geomorphology 374, 107516. https://doi.org/10.1016/j.geomorph.2020.107516

Sáez, A., Carballeira, R., Pueyo, J.J., Vázquez-Loureiro, D., Leira, M., Hernández, A., Valero-Garcés, B.L., Bao, R., 2018. Formation and evolution of back-barrier perched lakes in rocky coasts: An example of a Holocene system in north-west Spain. Sedimentology 65, 1891–1917. https://doi.org/10.1111/sed.12451

Santos, Â., Mendes, S., Corte-Real, J., 2014. Impacts of the storm Hercules in Portugal. FIT 49. https://doi.org/10.18055/Finis6468

Small, C., Nicholls, R.J., 2003. A Global Analysis of Human Settlement in Coastal Zones. Journal of Coastal Research 19, 584–599.

Trigo, R.M., Valente, M.A., Trigo, I.F., Miranda, P.M.A., Ramos, A.M., Paredes, D., García-Herrera, R., 2008. The Impact of North Atlantic Wind and Cyclone Trends on European Precipitation and Significant Wave Height in the Atlantic. Annals of the New York Academy of Sciences 1146, 212–234. https://doi.org/10.1196/annals.1446.014

Vautard, R., Cattiaux, J., Yiou, P., Thépaut, J.-N., Ciais, P., 2010. Northern Hemisphere atmospheric stilling partly attributed to an increase in surface roughness. Nature Geoscience 3, 756–761. https://doi.org/10.1038/ngeo979

Vilas, F., Rolán, E., 1985. Caracterización de las lagunas costeras de Galicia, N.W. Peninsula Ibérica. España. Actas I^{o} Congreso Ibérico de Quaternario.

Villacieros-Robineau, N., Gilcoto, M., Pardo, P.C., Barton, E.D., 2021. Wave Regime and Wave-Current Coupling in an Upwelling–Driven Bay: Seasonal and Inter-Annual Variability. JGR Oceans 126, e2021JC017540. https://doi.org/10.1029/2021JC017540

Vousdoukas, M.I., Mentaschi, L., Voukouvalas, E., Verlaan, M., Feyen, L., 2017. Extreme sea levels on the rise along Europe's coasts. Earth's Future 5, 304–323. https://doi.org/10.1002/2016EF000505

Vousdoukas, M.I., Ranasinghe, R., Mentaschi, L., Plomaritis, T.A., Athanasiou, P., Luijendijk, A., Feyen, L., 2020. Sandy coastlines under threat of erosion. Nature Climate Change 10, 260–263. https://doi.org/10.1038/s41558-020-0697-0

Walsh, K.J.E., McBride, J.L., Klotzbach, P.J., Balachandran, S., Camargo, S.J., Holland, G., Knutson, T.R., Kossin, J.P., Lee, T., Sobel, A., Sugi, M., 2016. Tropical cyclones and climate change. WIREs Climate Change 7, 65–89. https://doi.org/10.1002/wcc.371

Wohland, J., Folini, D., Pickering, B., 2021. Wind speed stilling and its recovery due to internal climate variability. Earth System Dynamics Discussions 1–27.

Zarnetske, P.L., Ruggiero, P., Seabloom, E.W., Hacker, S.D., 2015. Coastal foredune evolution: the relative influence of vegetation and sand supply in the US Pacific Northwest. Journal of the Royal Society Interface 12, 20150017. https://doi.org/10.1098/rsif.2015.0017

Zeng, Z., Ziegler, A.D., Searchinger, T., Yang, L., Chen, A., Ju, K., Piao, S., Li, L.Z.X., Ciais, P., Chen, D., Liu, J., Azorin-Molina, C., Chappell, A., Medvigy, D., Wood, E.F., 2019. A reversal in global terrestrial stilling and its implications for wind energy production. Nature Climate Change 9, 979–985. https://doi.org/10.1038/s41558-019-0622-6

Zhang, Z., Wang, K., Chen, D., Li, J., Dickinson, R., 2019. Increase in Surface Friction Dominates the Observed Surface Wind Speed Decline during 1973–2014 in the Northern Hemisphere Lands %J Journal of Climate. Journal of Climate 32, 7421–7435. https://doi.org/10.1175/jcli-d-18-0691.1

ABSTRACT

Coastal dunes evolve in direct response to primary drivers, such as wind and waves, which can significantly influence the landscape. Here, we examine the effects of the wind and wave regimes on the vegetation cover and shoreline position of the dune system that makes up the Doniños barrier on the rocky NW Iberian coast since the middle of the 20th century. By studying a series of aerial images, we determined that the vegetated dunes experienced net seaward shoreline advance at an average rate of 1.28±0.01 m/year and an overall dune vegetation coverage expansion of 50.5%. Available local atmospheric data indicated that wind stilling was the main factor responsible for these trends. However, the shoreline evolution process included annual-to-decadal periods dominated by stalled or reversed advances in energetic winters when waves could reach the foredune, causing erosion and vegetation cover deterioration. Consecutive energetic winters resulted in severe foredune erosion and slow to no recovery of shoreline advance thereafter. This work presents a case study in which a new conceptual model of the opposite and unbalanced effects of wind stilling and storm surges on foredune evolution dynamics is discussed and established under the current climate change scenario

HIGHLIGHTS

- The post-mid-20th-century stabilization of coastal dunes by vegetation was triggered by wind stilling.
- Vegetation cover expansion has made the system more resistant to marine erosion, allowing a net seaward shoreline advance.
- Wind stilling can also reduce the foredune profile recovery capacity due to the decrease in the beach-to-dune sand transfer capacity of wind.
- The recurrence of energetic winters provokes the stalling or reversal of foredune recovery.